Magnetic Transitions of Superconducting Thin Films and Foils. II. Tin

R. E. MILLER AND G. D. CODY
RCA Laboratories, Princeton, New Jersey
(Received 27 February 1968)

The perpendicular and parallel magnetic critical fields of pure tin films and foils have been measured as a function of temperature (1.3°K–T_c) and specimen thickness (500 Å–220 kÅ). The critical field $H_\perp$ for specimens of thickness less than a critical thickness d_c is in good agreement with Tinkham's vortex model for thin films if one assumes a thickness dependence for the penetration depth. For thicker films and foils the observed thickness dependence of $H_\perp$ is in good agreement with a theory based on the effect of positive surface energy on the free energy of the intermediate state. The measured parallel critical field $H_{||}$ is in excellent agreement with Ginzburg-Landau theory for type-I superconductors in both the thin- and thick-film limits. For films thinner than a critical thickness d_c', the transition is of second order and the relationship between $H_\perp$, $H_{||}$, and the film thickness is in excellent agreement with the "universal curve" of Saint James and de Gennes for second-order transitions. For films thicker than d_c', the transitions are of first order, and the critical fields approach the Ginzburg-Landau limit valid for $d \gg \lambda$. A comparison of the observed critical thicknesses d_c and d_c' with theoretical calculations has been made. From the data, bulk values for $\kappa(t)$, $\lambda(t)$, $\lambda_L(0)$, ξ_0, and Δ have been computed, and the thickness dependence of $\kappa(t)$ and $\lambda(t)$ has been estimated.

I. INTRODUCTION

WE have made measurements of the perpendicular and parallel magnetic critical fields of films and foils of pure tin. The measurements covered the thickness range 500 Å to 220 kÅ and a temperature range from 1.3°K to the critical temperature of the specimens. The experimental techniques in these measurements are identical to those of the preceding paper,[1] which we will hereafter refer to as I, but the results differ significantly from those obtained for lead. However, the observed differences can be satisfactorily accounted for by current theories of thin-film behavior.

A variety of measurements of the critical fields of tin have been reported by numerous workers,[2–11] each set of measurements covering a limited thickness range and usually only one field orientation. The reported results on perpendicular critical fields are particularly confusing and might lead one to the conclusion that the transition from thin-film to thick-film behavior is discontinuous.[2,3,10] We have covered a wide enough range of specimen thickness to clarify this point and in addition have made measurements in both the perpendicular and parallel field orientations on the same specimens. In general, we have found that the agreement of theory with our results is good, and the agreement of derived parameters with independent measures of the same quantities is satisfactory.

II. EXPERIMENTAL PROCEDURE

A. Sample Preparation and Description

Evaporated films were utilized to study the thickness range 500 Å–44 kÅ. They were prepared by evaporating 99.999% tin onto liquid-N_2-cooled glass substrates (Corning 7059) at a typical pressure of about 8×10^{-7} mm Hg and at a deposition rate of about 75 Å/sec. In some cases the deposited films had an under and over layer of evaporated SiO to simulate conditions of typical device geometries. The thicknesses of the films were determined by means of periodic interferometric measurements and crystal-thickness monitor readings.

The films were found to have critical temperatures ranging from 3.83–3.92°K. T_c was determined by extrapolating the parallel field data to zero field. In these measurements the earth's field was not nulled but had a very small (<0.005°K) effect on the transition temperature as determined in this manner. The effective transition width was about 10–15 mdeg. As was previously found for tin films by other workers including Blumberg and Seraphim,[12] the films showed a weak inverse thickness dependence of T_c. There was considerable scatter in T_c despite our efforts to duplicate deposition conditions for each film. The use of SiO layers on some films apparently did not influence T_c or other properties of these films when compared to films without SiO. Figure 1 shows the measured critical temperatures as a function of film thickness.

Foils rolled from the same 99.999% tin were utilized to study the thickness range 60–220 kÅ. The thickness

[1] G. D. Cody and R. E. Miller, preceding paper, Phys. Rev. **173**, 481 (1968). See also G. D. Cody and R. E. Miller, Phys. Rev. Letters **16**, 697 (1966).
[2] J. P. Burger, G. Deutscher, E. Guyon, and A. Martinet, Phys. Rev. **137**, A853 (1965).
[3] E. H. Rhoderick, Proc. Roy. Soc. (London) **A267**, 231 (1962).
[4] E. Guyon, C. Caroli, and A. Martinet, J. Phys. (Paris) **25**, 683 (1964).
[5] J. M. Lock, Proc. Roy. Soc. (London) **A208**, 391 (1951).
[6] D. H. Douglas, Jr., and R. H. Blumberg, Phys. Rev. **127**, 2038 (1962).
[7] J. P. Baldwin, Rev. Mod. Phys. **36**, 317 (1964).
[8] D. R. Tilley, J. P. Baldwin, and G. Robinson, Proc. Phys. Soc. (London) **89**, 645 (1966).
[9] G. Robinson, Proc. Phys. Soc. (London) **89**, 633 (1966).
[10] E. A. Davies, Proc. Roy. Soc. (London) **A255**, 407 (1960).
[11] E. R. Andrew and J. M. Lock, Proc. Roy. Soc. (London) **A63**, 13 (1949).
[12] R. H. Blumberg and D. P. Seraphim, J. Appl. Phys. **33**, 163 (1962).

of each foil was determined by weighing. The geometry of all specimens was that of a disk $\frac{7}{16}-\frac{1}{2}$ in. diam.

B. Critical-Field Measurements

1. Magnetization Measurements in Transverse Fields

Magnetization measurements in perpendicular fields were carried out using a standard flux-change technique which is described in I. The magnetization curves observed were used to obtain the perpendicular critical fields $H_\perp$ (defined by $M=0$) and other pertinent information concerned with the shape of the curves and the magitude of the magnetization M.

2. Susceptibility Measurements

The critical fields of all specimens in a parallel field and of thin specimens in a perpendicular field were determined by means of an ac bridge technique which monitors the complex susceptibility of the specimen. This technique was also employed to determine the critical temperature T_c of each specimen. The description of this technique and its theoretical justification has been discussed previously in I.

C. Resistance Measurements

1. Thick Foils

Standard four-terminal dc resistance measurements were made on two tin foils of thickness 126 and 220 kÅ at 300 and 4.2°K. In addition, the resistivities of these foils and four others, ranging in thickness from 69 to 220 kÅ, were determined at 4.2°K by ac susceptibility measurements on the foils in the normal state. This technique of determining resistivities of thin films and foils has been described in I. The results of both the dc and ac measurements are shown in Fig. 2, where the resistivity at 4.2°K, $\rho_{4.2}$, has been plotted as a function of the inverse thickness $1/d$ of the foils. If one assumes

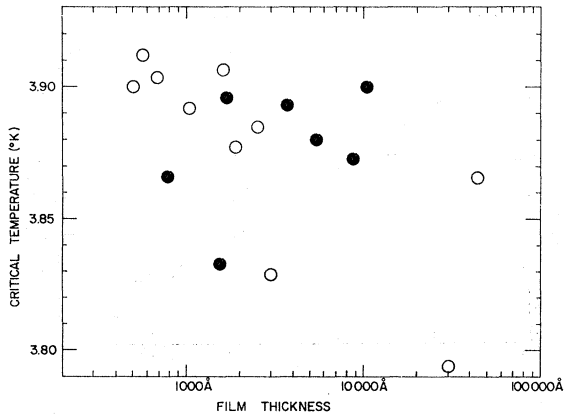

FIG. 1. Critical temperature of Sn films as a function of film thicknesses. Dark circles indicate films with SiO coatings. Transition widths were about 10–15 mdeg.

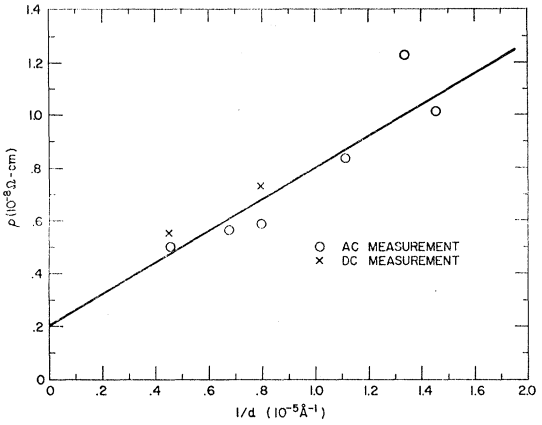

FIG. 2. Resistivity of Sn foils as a function of inverse thickness.

the thick-film approximation of Fuchs,[13] the intercept and slope of the best-fitting straight line through the data leads to a value of 2.0×10^{-9} Ω cm for the resistivity of a bulk specimen $\rho_{\infty\ 4.2°}$ and a bulk mean free path of ≈800 kÅ. The $[\rho l]_{4.2°}$ product is then $\approx1.6\times10^{-11}$ Ω cm², a value in good agreement with others.[6] The observed resistance ratios $R_{300}/R_{4.2}$ from the dc measurements were about 2000.

2. Thin Films

The dc resistances of six films ranging in thickness from 680 to 10 400 Å were determined by standard means at 300 and 4.2°K. The films were chosen from specimens which had previously been studied by magnetization and ac susceptibility techniques. The resistivity results at 4.2°K were more scattered than the foil results but lead to an effective bulk mean free path of 10 000–20 000 Å. The observed resistivity ratios $R_{300}/R_{4.2}$ were typical of values reported by others.[3] For a 1000-A film $R_{300}/R_{4.2}=15$, for a 10 000-Å film $R_{300}/R_{4.2}=55$.

III. EXPERIMENTAL RESULTS

A. Magnetization Curves

Magnetization measurements in perpendicular fields were made on 21 specimens covering the thickness range 500 Å–220 kÅ. The magnetization curves can be divided into two distinct thickness ranges (an observation that was noted also for Pb films in I). Figures 3(a)–3(c) show the magnetization curves for typical tin specimens at various temperatures. In Fig. 3(a) the magnetization curve for a 3000-Å film is typical of all films of thickness less than a critical thickness d_c which is found experimentally to be a function of temperature. The shape of the curve closely resembles the magnetization curves of tin films obtained by Robinson[9] and Chang *et al.*[14]

[13] K. Fuchs, Proc. Cambridge Phil. Soc. **34**, 100 (1938).
[14] G. K. Chang, T. Kinsel, and B. Serin, Phys. Letters **5**, 11 (1962).

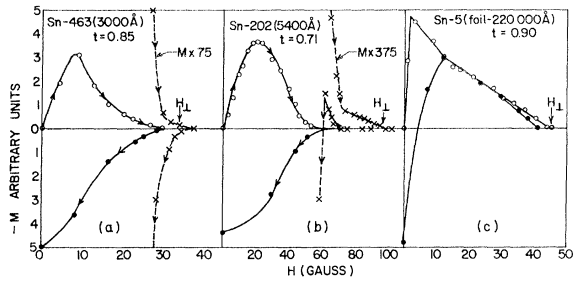

FIG. 3. (a) Magnetization curve for a 3000-Å Sn film at a reduced temperature of $t=0.85$. (b) Magnetization curve for a 5400-Å Sn film at a reduced temperature of $t=0.71$. (c) Magnetization curve for a 220-kÅ Sn foil at a reduced temperature of $t=0.90$.

In Fig. 3(b) the curve for a 5400-A film shows the first observable features of an intermediate-state behavior. Near $H_\perp(M\to 0)$ the magnetization approaches zero in increasing fields linearly, in contrast to the near parabolic approach of films for which $d<d_c$. The value of the slope in this linear region, dM/dH, is in good agreement with the expected value for a disk in a superconducting intermediate state. We shall discuss this point in detail in a later section. The 5400-Å film was the thinnest film to exhibit this linear behavior near $H_\perp$, and it did not show it above a reduced temperature $t>0.90$.

In Fig. 3(c) the curve for a 220 kÅ foil closely resembles the magnetization curves of Andrew and Lock[11] for tin foils. Here we seen that intermediate-state behavior sets in at a relatively small fraction of the critical field. Again the observed slope in the intermediate-state region is in good agreement with its expected value.

In contrast to magnetization curves for thick Pb films and foils (see I), we notice a "supercoolinglike" hysteresis in Figs. 3(b) and 3(c). The magnetization remains zero in decreasing fields to fields below $H_\perp$ (which is defined in increasing fields). This behavior is not yet understood, but it is not observed in films of thickness $d<d_c$. While for the thickest foils measured the hysteresis could possibly be a supercooling towards H_{c3}, for less thick films and foils $H_{c3}=1.7\sqrt{2}\kappa H_c$ would be greater than $H_\perp$. Andrew and Lock[11] have reported similar "supercooling" behavior for tin foils.

B. Susceptibility Data

As was stated earlier, ac susceptibility data were taken to obtain the parallel critical field $H_{||}$ over the entire range of thickness and temperature covered. In addition, this technique was utilized to obtain values of $H_\perp$ for films $d<d_c$. Figure 4 shows typical results of $H_\perp$ and $H_{||}$ determinations from susceptibility measurements as a function of temperature near T_c for a 1700-A tin film. For convenience we have plotted $H_{||}^2$ rather than $H_{||}$. As in I it is necessary to introduce an additional critical thickness d_c', for the parallel data. For films of thickness greater than the critical thickness d_c', we observed a field hysteresis in the parallel-field ac susceptibility data. As in I, we denote the parallel critical field when hysteresis was observed by the first-order critical field $H_{||}'$. We thus associate the hysteresis with supercooling towards the second-order transition field $H_{||}$. The hysteresis was typically 5–12% of $H_{||}'$. When hysteresis was observed ($d>d_c'$) the critical field shown in the figures is $H_{||}'$.

C. Resistive Transition Data

In order to compare our definitions of $H_\perp$ and $H_{||}$ as obtained from magnetization and ac susceptibility measurements with those of others who have used resistance transitions to define the critical fields, the resistance transitions of several films were determined in perpendicular and parallel magnetic fields at several temperatures. The results of some of these measurements on a 1700-Å film and a 10 400-Å film in perpendicular fields are shown in Fig. 5, along with magnetization and susceptibility results obtained earlier on the same films. We can make several important observations from these results:

(1) For the thin 1700-Å film which showed a second-order transition in a perpendicular field by magnetization measurements, the different measurements of $H_\perp$ are in essential agreement if $H_\perp$ is defined as either the field corresponding to the magnetization, $M\to 0$, the maximum in the imaginary part of the complex susceptibility of the sample coil, or the *onset* of dc resistance of the specimen.

(2) We note also for the 1700-Å film that the full value of the film's normal resistance is not restored until an applied field of about $1.7H_\perp$ is applied. This strongly suggests we are observing surface superconductivity on the edge at fields greater than $H_\perp$ and that the field at which normal resistance is restored corresponds to H_{c3}. This observation is consistent with microwave-resistance

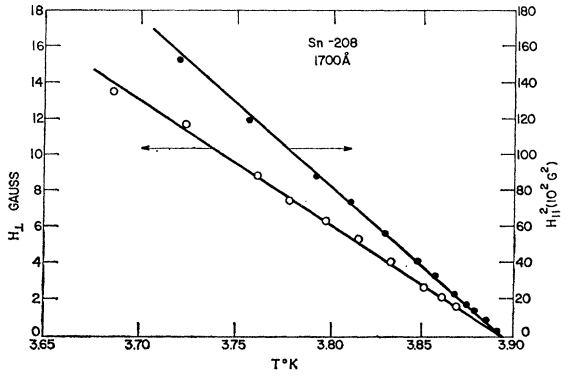

FIG. 4. Results for the critical fields $H_\perp$ and $H_{||}$ at T near T_c as determined from ac susceptibility measurements on a Sn film 1700 Å thick.

measurements on thin tin and indium films by Gittleman *et al.*[15]

(3) For the thicker 10 400-Å film which showed intermediate-state behavior in perpendicular fields just below $H_\perp$ in magnetization measurements, $H_\perp$ as defined from magnetization measurements ($M \to 0$) corresponds to a nearly complete restoration of the normal resistance of the film. The resistance observed at much lower fields than $H_\perp$ may be attributed to flux-flow resistance since we believe the film to be in an intermediate state. The occurence of the maximum in the imaginary part of the complex susceptibility at considerably lower fields than $H_\perp$ is consistent with this reasoning (see I).

(4) Another observation is that considerable hysteresis is found in the R-versus-H curve for the 10 400-Å film. This is consistent with hysteresis found in the magnetization and ac susceptibility data for thick films. No hysteresis is observed for the 1700-Å film.

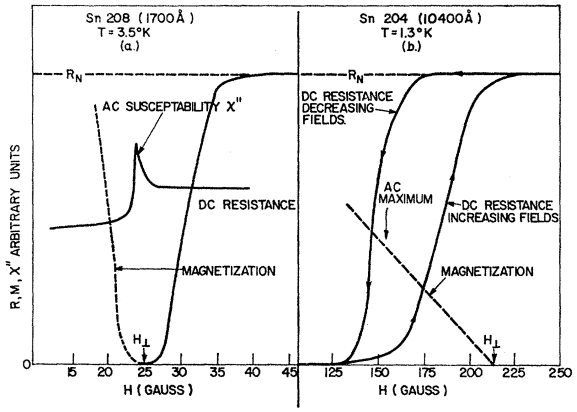

FIG. 5. (a) Perpendicular magnetic transition of a thin film (1700 Å) at 3.5°K as determined from magnetization, ac susceptibility, and dc resistance measurements. (b) Perpendicular magnetic transition of a thick film (10 400 Å) at 1.3°K as determined by magnetization and dc resistance measurements. Arrow indicates position of maximum observed on imaginary part of ac susceptibility.

The resistive transitions in parallel fields were in all cases sharp and the agreement of the field corresponding to $R/R_N = \frac{1}{2}$ (used to define $H_{||}$ by most workers), with the value determined from ac susceptibility measurements, was within about 5%. Hysteresis loops very much like those observed by Tilley[8] were found for the 10 400-Å film. No hysteresis was observed for the thinner films. This is again consistent with the ac susceptibility results which showed no hysteresis for films $d < d_c'$.

D. Critical Fields

Figures 6 and 7 show $H_\perp$ and $H_{||}$ as a function of temperature on two films 1040 Å and 10 400 Å thick, respectively. The differences in the temperature dependences of the critical fields for a thin versus a thick specimen are clearly illustrated but we will defer discussion to a later section. From plots such as these, we have prepared Fig. 8(a)–8(e), which shows the thickness dependences of the reduced critical fields $H_\perp/H_c$ and $H_{||}/H_c$. For convenience we have chosen to display these data at five reduced temperatures. Use of the reduced fields and reduced temperatures has been made to circumvent effects of differences in the critical temperatures of the specimens.

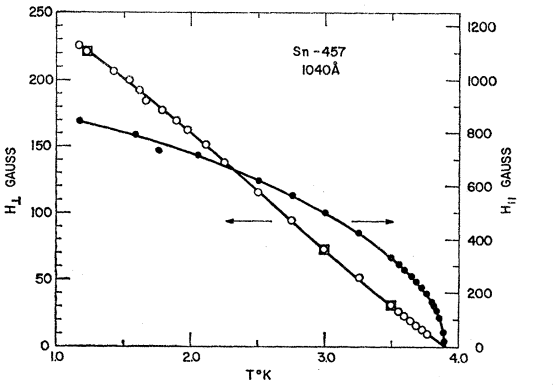

FIG. 6. Complete critical-field results as a function of temperature on a 1040-Å Sn film from magnetization (squares) and ac susceptibility data (circles).

The bulk critical-field data of Shaw *et al.*[16] and the correspondence principle, $H_c(0)/T_c = \text{const}$, have been used to calculate $H_c(t)$ for each specimen. The general features of the curves are (1) a minimum in $H_\perp/H_c$ which shifts to lower values of d as the temperature is reduced; (2) a sharp rise in both $H_\perp/H_c$ and $H_{||}/H_c$ for

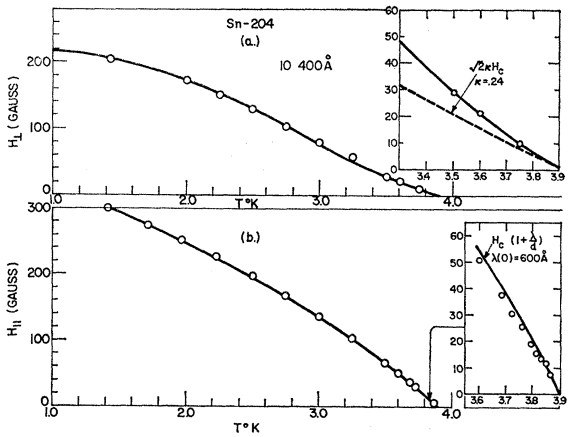

FIG. 7. Complete critical-field results as a function of temperature on a 10 400-Å Sn film. (a) $H_\perp$ from magnetization measurements. Dashed curve is from Eq. (6), which should be valid very near T_c. (b) $H_{||}$ from ac susceptibility measurements. Solid curve in blown-up section near T_c shows fit to Ginzburg-Landau theory for thick films.

[15] J. I. Gittleman, S. Bozowski, and B. Rosenblum, Phys. Rev. **161**, 398 (1967).

[16] R. W. Shaw, D. E. Mapother, and D. C. Hopkins, Phys. Rev. **120**, 88 (1960).

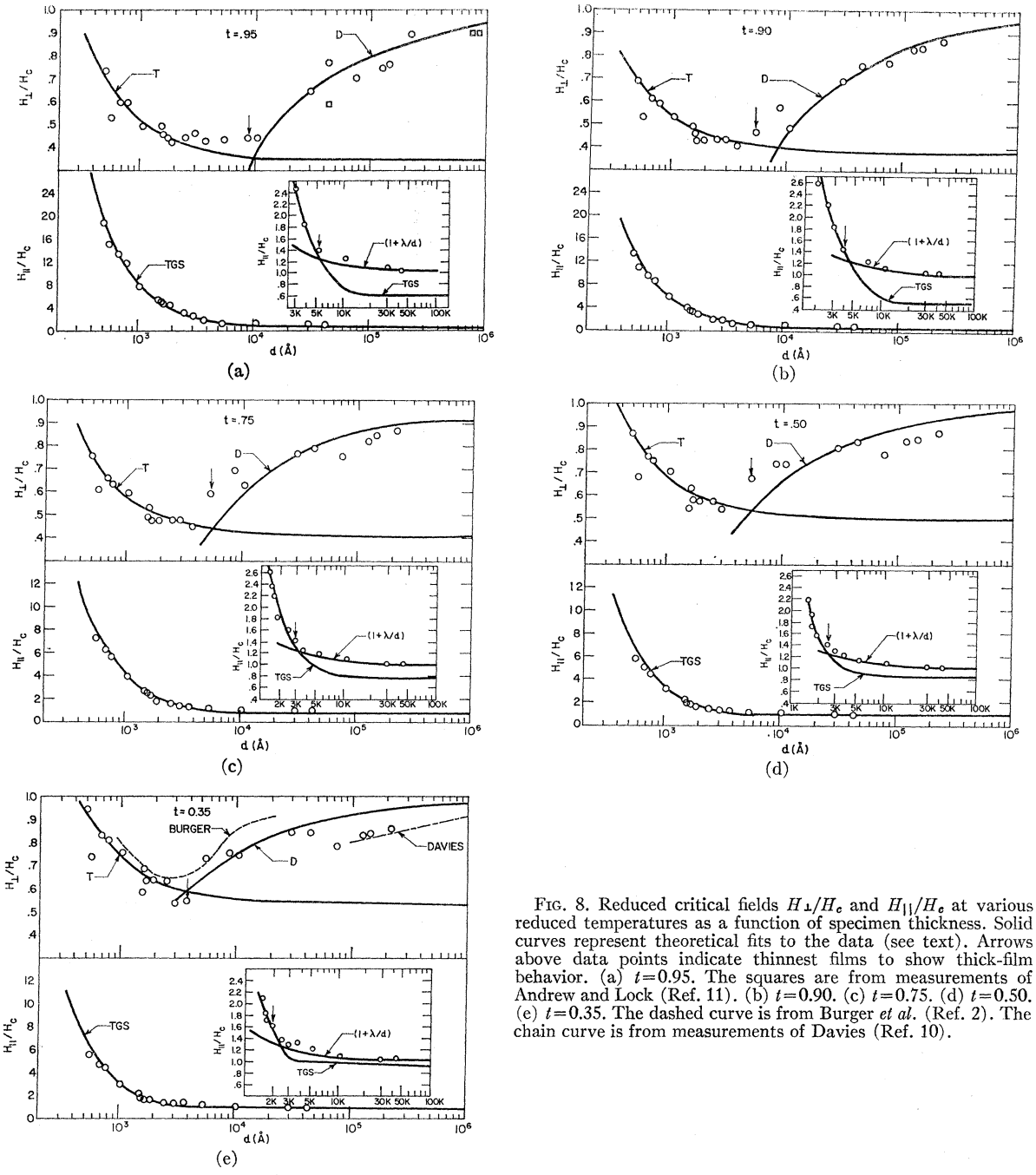

FIG. 8. Reduced critical fields $H_\perp/H_c$ and $H_{||}/H_c$ at various reduced temperatures as a function of specimen thickness. Solid curves represent theoretical fits to the data (see text). Arrows above data points indicate thinnest films to show thick-film behavior. (a) $t=0.95$. The squares are from measurements of Andrew and Lock (Ref. 11). (b) $t=0.90$. (c) $t=0.75$. (d) $t=0.50$. (e) $t=0.35$. The dashed curve is from Burger *et al.* (Ref. 2). The chain curve is from measurements of Davies (Ref. 10).

small d; (3) a gradual approach to unity for both $H_\perp/H_c$ and $H_{||}/H_c$ (bulk behavior) for large d. Included in the figures are lines corresponding to theoretical fits and these will be discussed later. In each figure arrows have been placed to indicate the thinnest films which show thick-film behavior. In perpendicular fields, we define thick films as those which have a linear slope in their magnetization curves near $H_\perp$ (i.e., $d>d_c$). In parallel fields, thick films are those which exhibit field hysteresis (i.e., $d>d_c'$). Also shown are critical-field data of other workers for comparison (see figure captions).

E. Comparison of Critical-Field Results

1. $H_\perp$—Thin Films

Rhoderick[3] reports critical fields on thin tin films in perpendicular fields which are 1.4–2 times greater than the present observations. The discrepancy is surely due to his definition of $H_\perp$ as the field corresponding to

complete restoration of resistance. As we have noted earlier, this definition probably corresponds to H_{c3}, not $H_\perp$. Burger *et al.*[2] have reported values for $H_\perp$ for tin films at 1.6°K obtained from tunneling and resistance measurements. As we see in Fig. 8(e) the agreement with our data is satisfactory, although their results are somewhat higher than this work. Their values of $H_\perp$ from resistance measurements were defined as the fields corresponding to $R/R_N=\frac{1}{2}$. Their results show the same minimum in $H_\perp$ versus d as this work.

2. $H_\perp$—*Thick Foils*

Andrew and Lock[11] and Davies[10] have reported critical-field determinations on thick foils of tin in perpendicular fields. Andrew and Lock obtained their results from magnetization measurements in much the same manner as has been reported here. Some of their results are shown in Fig. 8(a). The agreement with these measurements is seen to be within the experimental scatter of our data. Davies obtained somewhat lower values of $H_\perp$ [see Fig. 8(e)] from resistance measurements. Presumably this is due to his definition of $H_\perp$ as the point where the resistance in an increasing field starts to saturate. Resistance transition measurements made on two of our foils showed that to within 2–3%, the value of $H_\perp$ obtained from $M\to 0$ corresponded to that obtained from $R/R_N\to 1$ [Fig. 5(b)].

3. *Parallel Data*

In Fig. 9 we show the results of critical-field determinations at $t=0.95$ on tin films in parallel fields by resistance measurements of several other workers[3,6,7] along with a smooth curve corresponding to this work. The agreement is seen to be good except at thicknesses $d<1000$ Å. In this range the data of Blumberg and Douglas[6] is 20–30% higher than this work. Their data seems to approach ours at a thickness of about 1000 Å. This difference is not understood.

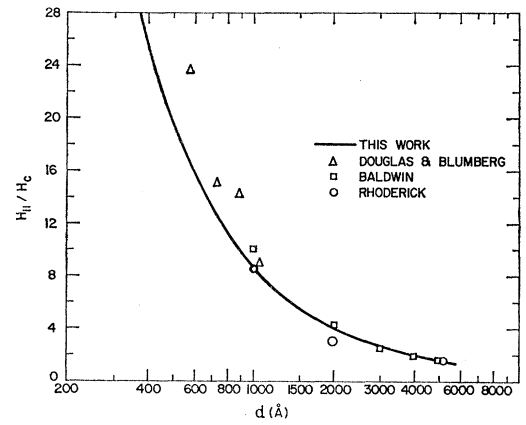

FIG. 9. Comparison of our parallel field results at $t=0.95$ with those of Refs. 3, 6, and 7.

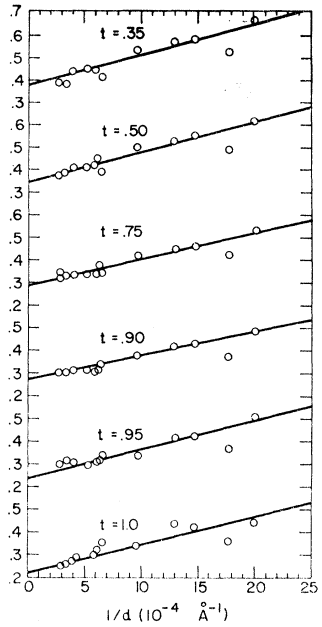

FIG. 10. Thickness dependence of κ at reduced temperatures $t=0.35$, 0.50, 0.75, 0.90, 0.95, and 1.0.

IV. DISCUSSION

A. Perpendicular Critical Fields, Thin Films

As discussed in I for thin films which undergo a second-order transition in perpendicular fields, a reasonable approximation for the perpendicular critical fields are given by Tinkham's[17,18] expression

$$H_\perp(t,d)=\sqrt{2}\,\kappa(t,d)H_c(t), \tag{1}$$

where the thickness-dependent κ can be written as

$$\kappa(t,d)=\kappa_\infty(t)[1+b(t)/d]. \tag{2}$$

$\kappa_\infty(t)$ is the bulk value of the Ginzburg-Landau parameter, $H_c(t)$ is the bulk critical field, and t is the reduced temperature. The quantity $b(t)$ is given by

$$b(t)=\tfrac{3}{8}[\lambda_L^2(t)\xi_0/\lambda_\infty^2(t)]. \tag{3}$$

At low temperatures, if we use the literature[19] values for ξ_0 and λ_∞/λ_L (2300 Å and 1.57, respectively), we obtain for $b(0)$ a value of 350 Å. At T_c where $\lambda_\infty=\lambda_L$, we obtain $b(1)=860$ Å.

From plots like Fig. 4 prepared for each thin-film specimen, $d<d_c$, we have obtained experimental values of $\kappa(T_c,d)$ from the relation

$$\kappa(1,d)=\lim_{t\to 1}\sqrt{2}^{-1}(dH_\perp/dt)\,(dH_c/dt). \tag{4}$$

Values of dH_c/dt were obtained from the data of Shaw

[17] M. Tinkham, Phys. Rev. **129**, 2413 (1963).
[18] M. Tinkham, Rev. Mod. Phys. **36**, 268 (1964).
[19] J. Bardeen and J. R. Schrieffer, in *Progress in Low Temperature Physics*, edited by C. J. Gorter (North-Holland Publishing Co., Amsterdam, 1961), Vol. 3, p. 243.

TABLE I. Thickness and temperature dependence of κ for tin.

t	1.0	0.95	0.90	0.75	0.50	0.35	0
κ_∞	0.22	0.24	0.27	0.29	0.34	0.38	0.44[a]
b(Å)	570	540	398	403	388	355	
b(Å)[b]	860						350

[a] Extrapolated value from two-fluid model. [b] From Eq. (3).

et al.[16] At other temperatures we have obtained experimental values of $\kappa(t, d)$ directly from Eq. (1) and the measured values of $H_\perp$. In Fig. 10 the values of $\kappa(t, d)$ obtained from Eqs. (1) and (4) have been plotted as a function of $1/d$ at $t=1$, 0.95, 0.90, 0.75, 0.50, and 0.35. From best straight-line fits to the points, we have obtained values of $\kappa(t, \infty)$ and $b(t)$. The results are given in Table I along with the calculated estimates of $b(t)$ from Eq. (3). The agreement of the experimental value of b at low temperatures with the calculated estimate is remarkably good, while at T_c the experimental result is somewhat low. The observed temperature dependence of $b(t)$ is about as expected since the ratio λ_∞/λ_L should not vary much until very near T_c. We have observed similar agreement at low temperatures for Pb films (I). $\kappa(1, \infty)$ is somewhat higher than values obtained experimentally on bulk specimens[20,21] but is not much different from values obtained by others from thin-film results.[8,14]

In Fig. 11 we have plotted the extrapolated values of $\kappa(t, \infty)$ obtained from Fig. 10 as a function of the reduced temperature. A solid curve corresponding to the Gorter-Casimir two-fluid temperature dependence for κ, $\kappa(t)=\kappa(0)(1+t^2)^{-1}$, has been drawn fitted to the experimental point at T_c. As can be seen the data gives a fair fit to this dependence on t. The two-fluid model leads to a value of $\kappa(0, \infty)$ of 0.44.

The solid lines labeled T drawn through the thin-film $H_\perp$ data in Fig. 8 were drawn using Eq. (1) and the parameters $\kappa(t, d)$ and $b(t)$ from Table I. One observes that the fit to the thin-film region is satisfactory.

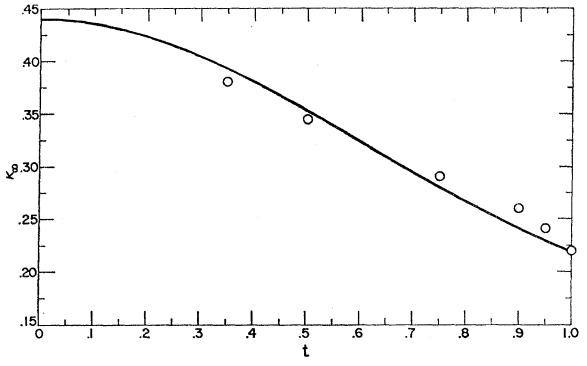

FIG. 11. $\kappa(t, \infty)$ as a function of t. Smooth curve is based on two-fluid model. $\kappa(t, \infty)=\kappa(0, \infty)(1+t^2)^{-1}$.

[20] T. E. Faber, Proc. Roy. Soc. (London) **A241**, 531 (1957).
[21] F. W. Smith and M. Cardona, Phys. Letters **24A**, 247 (1967).

B. Perpendicular Critical Fields, Thick Films

As the thickness of the film increases beyond some critical thickness d_c, the intermediate state should become the stable state prior to the transition to the normal state. Guyon *et al.*[4] have calculated that the effect of the positive surface energy is to depress the transiton below H_c to a field $H_\perp^D$ given by

$$H_\perp^D=H_c[1-(C\Delta/d)^{1/2}], \tag{5}$$

where Δ is the surface-energy parameter and C is a constant which, depending on the particular geometrical model chosen to describe the intermediate state may have values, 0.8–2. We have found that a value for C of about 1 was necessary to describe our results for Pb (I). Our results for thick tin films and foils have been fitted to Eq. (5) by choosing a best value for Δ at each temperature and assuming $C=1$. The curves labeled D drawn through the $H_\perp/H_c$ data in Fig. 8 show the resultant fits.

In Fig. 12 we have plotted the values of Δ used to fit the $H_\perp/H_c$ data as a function of t along with theoretical curves derived from calculations of Bardeen[22] and Ginzburg.[23] These calculations give Δ/λ_∞ as a function

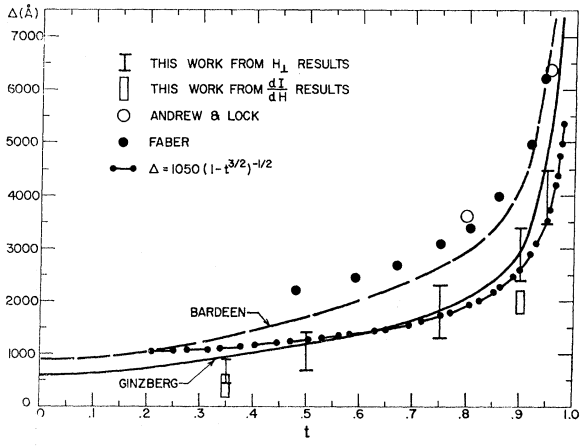

FIG. 12. Surface-energy parameter Δ as a function of temperature as determined from $H_\perp$ measurements on thick films [Eq. (5)] assuming $C=1$, and from the magnitude of the gradient of magnetization curves of thick films near $H_\perp$ [Eq. (6)]. Also shown are theoretical curves of Bardeen and Ginzburg. Results of Andrew and Lock (Ref. 11) and Faber (Ref. 24) are included for comparison. The chain curve is the empirical temperature dependence, $\Delta=\Delta(0)(1-t^{3/2})^{-1/2}$ fitted to our data. See text.

[22] J. Bardeen, Phys. Rev. **94**, 554 (1964).
[23] V. L. Ginzburg, Physica **24**, S42 (1958).

of κ. To obtain $\Delta(t)$ we have inserted our experimental values for $\kappa(t, \infty)$ into their functions, $\Delta/\lambda_\infty(\kappa)$ to obtain $\Delta/\lambda_\infty(t)$, and then solved for $\Delta(t)$ by assuming $\lambda_\infty(0) = 600$ Å and $\lambda_\infty(t) = \lambda_\infty(0)(1-t^4)^{-1/2}$.

One might expect the theoretical curve based on Ginzburg's result to be valid only near T_c, and that based on Bardeen's calculation to have broader validity. It is clear from Fig. 12, however, that the Ginzburg curve fits the data to within the experimental error quite well over a wide temperature range, agreeing in magnitude as well as functional dependence, while Bardeen's curve is higher than the experimental values at all temperatures, though its functional dependence on t is similar.

Also shown in Fig. 12 are values of Δ for tin obtained by Faber[24] and Andrew and Lock.[11] Faber's values were obtained by studying the velocity of propagation of superconductivity in tin rods, while Andrew and Lock's values were obtained by examining the shape of magnetization curves on tin foils. While they report temperature dependences for Δ which are similar to what we observed, they obtain significantly higher values for Δ. Davies[10] also studied the temperature dependence of Δ. He used resistive transitive measurements on tin foils and a dimensional analysis to conclude that Δ varies as $\Delta = \Delta(0)(1-t^{3/2})^{-1/2}$, a verification of the dependence observed by Faber. His definition of $H_\perp$ from his resistance transitions was too arbitrary, however, to obtain meaningful absolute values for Δ. While we can see from Fig. 12 that the temperature dependence, $\Delta = \Delta(0)(1-t^{3/2})^{-1/2}$, is a fair fit to our data, we also can observe that the dependence obtained from Ginzburg theory is better.

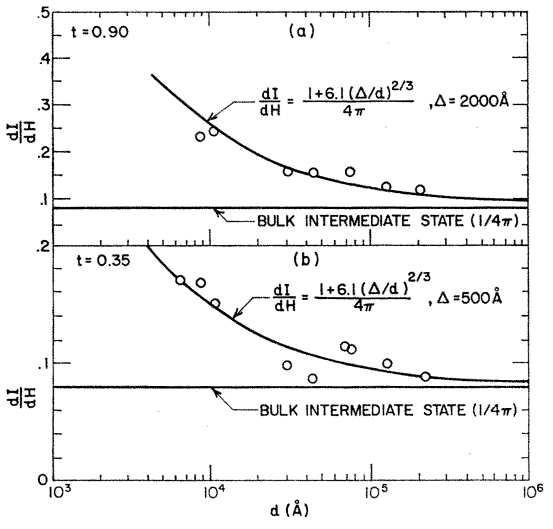

FIG. 13. Slope of magnetization curves, dI/dH, in linear region near $H_\perp$ as a function of specimen thickness. Solid curves are theoretical fits based on Eq. (6). (a) $t=0.90$. (b) $t=0.35$.

[24] T. E. Faber, Proc. Roy. Soc. (London) **A223**, 174 (1954).

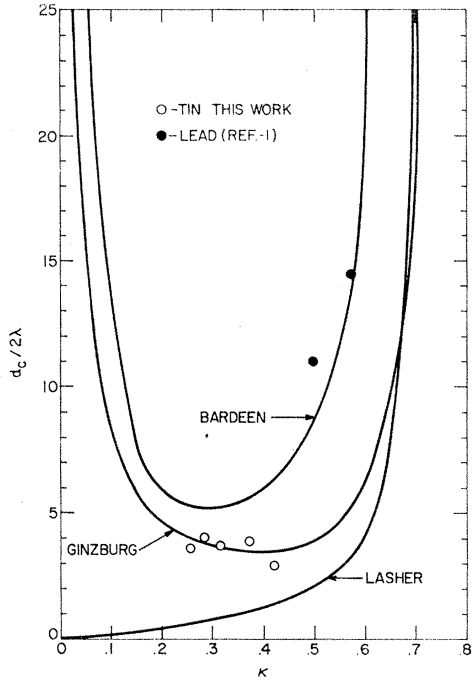

FIG. 14. The normalized critical thickness of tin and lead films, $d_c/2\lambda$, for the transition to the intermediate state as a function of κ. Solid curves are shown based on theoretical calculations of $\Delta/\lambda(\kappa)$ by Bardeen (Ref. 22), Ginzburg (Ref. 23), and Eq. (7) and also on Lasher's calculation of $d_c(\kappa)$ (Ref. 25).

We have also obtained values of Δ from our data in another semi-independent manner similar to the way Andrew and Lock obtained their values for Δ.[11] Andrew and Lock have calculated the effect that the positive surface energy of a superconducting ellipsoid in the intermediate state has on the slope of the magnetization curve. As discussed in I, the slope of the magnetization curve is given by

$$dI/dH = [1+6.1(\Delta/d)^{2/3}]/4\pi, \qquad (6)$$

where I is the magnetization per unit volume.

In Fig. 13 we have plotted the observed values of dI/dH for the films $d>d_c$ at reduced temperatures $t=0.90$ and 0.35 as a function of thickness. Through the experimental results we have drawn curves corresponding to Eq. (6) using values of Δ which gave the best fit to the experimental points. The values obtained for Δ are shown in Fig. 12. They are seen to be in fair agreement with our values obtained from $H_\perp$ data.

Having discussed the theoretical fits to both the thin-film and thick-film results for $H_\perp$, we can now obtain the critical thickness $d_c(t)$ by equating the expressions for $H_\perp/H_c$ for thin films, Eq. (1), and thick films, Eq. (5), $C=1$. Solving for $d=d_c$, we obtain

$$d_c(t) = \Delta(t)/[1-\sqrt{2}\,\kappa(t, d_c)]^2. \qquad (7)$$

In Fig. 14 we have plotted our experimental values for

TABLE II. Summary of results.

	This work							Source	Comparison
t	1.0[a]	0.95	0.90	0.75	0.50	0.35	0[a]		
Bulk κ	0.22	0.24	0.27	0.29	0.34	0.38	0.44	From $H_\perp$ results thin films	$\kappa(1, \infty)=0.15$[b] 0.15[c] 0.125[d]
Bulk λ[e] (Å)	...	1325	1025	725	620	600	600	From $H_\parallel$ results for λ_L of thin films	$\lambda(0)=560$ Å[b]
Δ (Å)	...	4000	2900	1750	1100	600	600	From $H_\perp$ results thick films	Agrees in value and temperature dependence with Ginzburg[f]
d_c (Å)	...	9700	8500	5600	5000	3600		From intersection of Eqs. (1) and (5)	Agrees with $d_c=\Delta/(1-\sqrt{2}\kappa)^2$ plus Ginzburg (Δ/λ).[f]
$\lambda_L(0, \infty)$ (Å)				422				From $H_\parallel$ results thin films	355[b]
ξ_0 (Å)				1800				$\lambda_L(0, \infty)/\kappa(T_c, \infty)$	2300[b]

[a] Extrapolated value.
[b] J. Bardeen and J. R. Schrieffer (see Ref. 19).
[c] G. K. Chang and B. Serin, Phys. Rev. **145**, 274 (1966).
[d] F. W. Smith and M. Cardonna (see Ref. 21).
[e] Assumes $\lambda(0)=600$ Å and $\lambda(t)=\lambda(0)(1-t^4)^{-1/2}$, $\lambda(0)=\sqrt{2}\lambda_L$.
[f] Reference 23.

$d_c/2\lambda$ as a function of κ, where d_c is the intersection of the curves T [Eqs. (1) and (2)] and D [Eq. (5)] in Fig. 8. The values of λ used are those given in Table II. The solid curves are from the theoretical work of Bardeen[22] and Ginzburg[23] for Δ/λ using Eq. (7), and from the exact calculation of $d_c(\kappa)$ by Lasher.[25]

For the Bardeen and Ginzburg theories there is an approximate symmetry about a minimum value of $d_c/2\lambda$ for $\kappa\approx 0.30$–0.35, while Lasher's calculation predicts that $d_c/2\lambda$ approaches zero with κ. Our results for tin seem to be in excellent agreement with Eq. (7) and Ginzburg's value for Δ/λ and much higher than Lasher's exact calculation. For comparison our results for lead films (I) have been included in the figure. They are in best agreement with the Bardeen result for Δ/λ. More data on type-I films such as indium or aluminum should confirm whether $d_c/2\lambda$ decreases for lower κ (Lasher) or rises [Eq. (7)].

C. Parallel Critical Fields, Thin Films

Ginzburg-Landau theory[26] predicts for thin superconducting films, $d<d_c'=\sqrt{5}\,\lambda$, in parallel fields, a second-order transition. Near T_c, the square of the critical field $H_{||}$ is given by

$$H_{||}^2(T, d) = 12[\lambda_L^2(0, d)/d]^2 T_c (dH_c/dT)_{T_c}^2 (T_c - T), \quad (8)$$

where $\lambda_L(0, d)$ is the thickness-dependent Landau penetration depth and we have utilized the Bardeen-Cooper-Schrieffer (BCS) expression for the temperature dependence of $\lambda(T, d)$.[27] From graphs like Fig. 4, where we have plotted $H_{||}^2$ as a function of T near T_c, we have determined $\lambda_L^2(0, d)$ using Eq. (8) and values of $(dH_c/dT)_{T_c}$ from Shaw.[16] Figure 15 shows the observed dependence of $\lambda_L^2(0, d)$ on the inverse film thickness $1/d$. Though we observe considerable scatter in the points, the dependence is linear. The solid line is a least-squares fit to the points. Furthermore, we can deduce by extrapolation values for the bulk London penetration depth $\lambda_L(0, \infty)$ and the parameter b near T_c. Based on the least-squares fit to the points, the values are $\lambda_L(0, \infty)=422$ Å, $b(T_c)=420$ Å. The observed value for $\lambda_L(0, \infty)$ is in fair agreement with the BCS estimate of 355 Å.[19] The value for $b(T_c)$ is about 25% lower than the value we determined from $H_\perp$ data

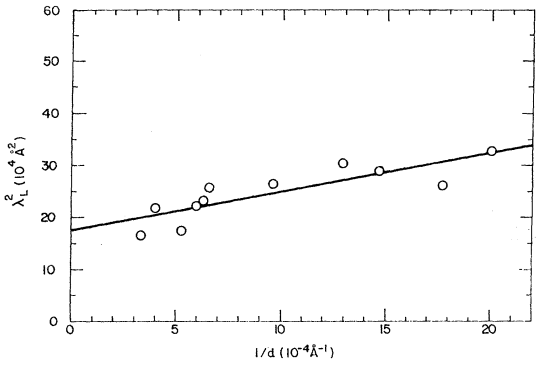

FIG. 15. Square of London penetration depth, λ_L^2, as a function of inverse film thickness. Solid line is least-squares fit to experimental points.

[25] G. Lasher, Phys. Rev. **154**, 153 (1967).
[26] V. L. Ginzburg and L. D. Landau, Zh. Eksperim. i Teor. Fiz. **20**, 1064 (1950).
[27] J. Bardeen, L. N. Cooper, and J. R. Schrieffer, Phys. Rev. **108**, 1175 (1957).

(Table I). The calculated value of $\lambda(0, \infty)$ is 600 Å, in agreement with values quoted by others.[7,28]

Since for thickness $d<d_c'$ the parallel transition is of second order, the critical fields should obey the "universal curve" of Saint James and de Gennes.[2,29] The solid curves through the $H_{||}/H_c$ data in Fig. 8 labeled TGS were computed from the Saint James–de Gennes "universal curve," the thickness of the films, and $H_\perp(t, d)$ as determined from Eqs. (1) and (2) and the experimental values of $\kappa_\infty(t)$ and $b(t)$ (Table I). The fit is seen to be remarkably good and strengthens the theoretical models we have chosen to fit both the perpendicular and parallel critical-field results for thin films.

D. Parallel Critical Fields, Thick Films

As we have said earlier, for thin enough films the transition in parallel fields is of second order and the critical fields are given by Eq. (8). However, for film thicknesses $d>d_c'$, the transition for tin ($\kappa<0.42$) should be first order, [1,26] and for $d\gg\lambda$, the fields will be given by

$$H_{||}'\approx H_c(1+\lambda/d). \tag{9}$$

In Fig. 6, we have used Eq. (9) to draw a solid curve through the parallel data near T_c for a 10 400-Å film which satisfies the thickness condition $d\gg\lambda$. We have assumed only that $\lambda(0)=600$ Å, a value derived from the thin-film parallel-field results, and $\lambda(t)=600(1-t^4)^{1/2}$. We see that the fit to the data is quite satisfactory.

In the inserts of Fig. 8 we have included theoretical curves corresponding to Eq. (9). Again we have assumed $\lambda(t)=600(1-t^4)^{-1/2}$. Small differences in λ due to its thickness dependence have been neglected. We clearly observe that the parallel critical field approaches the limiting expression for a first-order transition in a smooth fashion as d increases.

As we pointed out earlier the first-order transition fields can be distinguished from second-order fields by the presence of field hysteresis. Included in the inserts of Fig. 8 are arrows indicating the thinnest specimen to show field hysteresis. We see that these arrows are located at points where the data begin to deviate from the second-order TGS curves. From Ginzburg-Landau theory[26] the switch from second-order transition to first-order should occur at a critical thickness, $d_c'=\sqrt{5}\lambda$. This corresponds to a critical value of $H_{||}/H_c$ of about 2.2. We observe lower critical values of $H_{||}/H_c\approx$ (1.4–1.8). Whether this is a real deviation from theory or a lack of sensitivity is not clear, but the occurance of the arrows at just the point of departure from the TGS curve suggests a deviation from theory.

We observe also in the inserts that as t is reduced and κ increases, the second-order TGS curve is approaching the first-order curve. We would expect the two curves to cross at a value of $\kappa\approx0.42$ or at a temperature of about 1°K. Indeed for lead films (I), where $\kappa>0.42$ over the temperature range covered (1.4–4.2°K), first-order transitions were not observed but second-order transitions were ($H_{||}=H_{c3}>H_{||}'$).

V. CONCLUSIONS

We may summarize by drawing several conclusions from the experimental results:

(1) The perpendicular transition in the thin-film region up to a critical thickness d_c confirms Tinkham's prediction for a mixed state and the critical fields $H_\perp$ are given by Eq. (1).

(2) For thicknesses greater than d_c, the $H_\perp$ results are in fair agreement with a simple intermediate-state model based on the effect of the positive surface energy on $H_\perp$. We have obtained values of the surface-energy parameter Δ from the critical-field results and from the magnitude of the magnetization slope near $H_\perp$ which are in excellent agreement with each other and with Ginzburg-Landau theory.

(3) Values of the critical thickness d_c, which are obtained from the intersection of the theoretical expressions for the thin- and thick-films region, Eqs. (1) and (5), are in excellent agreement with theoretical values derived from intermediate-state (Davies) theory and exceed predicted values recently derived by Lasher. Additional data on type-I materials with lower values of κ might show whether the quantity $d_c/2\lambda$ begins to increase with decreasing κ as predicted by the intermediate-state model or to approach zero as predicted by Lasher.

(4) In parallel fields the critical fields are in excellent agreement with Ginzburg-Landau theory in both the thin- and thick-film limits. In addition, they are in agreement with the prediction of TGS for the relationship of $H_{||}$ with $H_\perp$ and film thickness for second-order transitions up to a critical thickness d_c'. For film thicknesses greater than d_c' the parallel transitions are first order, show field hysteresis (supercooling), and approach the Ginzberg-Landau limiting expression, $H_{||}'=H_c(1+\lambda/d)$, for films $d\gg\lambda$.

(5) We have also shown the danger of relying only on dc resistance measurements to define the critical fields. We now feel that this is the reason for the confusion which resulted when critical-field measurements of $H_\perp$ by several different workers were compared.

Finally we have prepared Table II which summarizes the values of the basic superconducting parameters, κ, λ, Δ, and ξ_0, which may be derived from our results and compares them with theoretical predictions.

ACKNOWLEDGMENTS

We are grateful to J. I. Gittleman for many helpful discussions and to S. Bozowski for preparing the film specimens.

[28] T. E. Faber and A. B. Pippard, Proc. Roy. Soc. (London) **A231**, 336 (1955).

[29] D. Saint James and P. G. de Gennes, Phys. Letters **7**, 306 (1963).